Synthesis and Luminescence Properties of New Blue-Light-Emitting Polyconjugated Poly{1,1′-biphenyl-4,4′-diyl-[1-(4-*t*-butylphenyl)]vinylene} Polymers and Copolymers

Chang-Gyu Kim,[1] Sung-Hoon Joo,[1] Cheol Hong Cheon,[1] Mi-Yun Jeong,[1] Soon-Wook Cha,[1] Byung-Hee Sohn,[2] Jung-Il Jin[1]

[1]*Department of Chemistry and Center for Electro- and Photo-Responsive Molecules, Korea University, Seoul 136-701, Korea*
[2]*Polymer Laboratory, Samsung Advanced Institute of Technology, Yongin-shi, Kyungki-do 449-901, Korea*

Received 14 January 2005; accepted 20 June 2005
DOI 10.1002/app.23109
Published online in Wiley InterScience (www.interscience.wiley.com).

ABSTRACT: Three new soluble polyconjugated polymers, all of which emitted blue light in photoluminescence and electroluminescence, were synthesized, and their luminescence properties were studied. The polymers were poly{1,1′-biphenyl-4,4′-diyl-[1-(4-*t*-butylphenyl)]vinylene}, poly((9,9-dioctylfluorene-2,7-diyl)-*alt*-{1,4-phenylene-[1-(4-*t*-butylphenyl)vinylene-1,4-phenylene]}) [P(DOF-PVP)], and poly([*N*-(2-ethyl) hexylcarbazole-3,6-diyl]-*alt*-{1,4-phenylene-[1-(4-*t*-butylphenyl)]vinylene-1,4-phenylene}). The last two polymers had alternating sequences of the two structural units. Among the three polymers, P(DOF-PVP) performed best in the light-emitting diode devices of indium–tin oxide/poly(ethylenedioxythiophene) doped with poly(styrene sulfonate) (30 nm)/polymer (150 nm)/Li:Al (100 nm). This might have been correlated with the balance in and magnitude of the mobility of the charge carriers, that is, positive holes and electrons, and also the electronic structure, that is, highest occupied molecular orbital (HOMO) and lowest unoccupied molecular orbital (LUMO) levels, of the polymers. © 2006 Wiley Periodicals, Inc. J Appl Polym Sci 100: 307–317, 2006

INTRODUCTION

Numerous polyconjugated polymers are known to exhibit photoluminescene (PL) and electroluminescence (EL) properties. Poly(*p*-phenylenevinylene) (PPV),[1–3] polyfluorene (PF),[4–6] and their derivatives[7–10] are representative examples. PPV is a green-light emitter, and PF is a blue-light emitter. Such light-emitting polymers can be used in the fabrication of polymer light-emitting diode (LED) devices, which are presently attracting a great deal of interest, especially for the possible development of new display materials and techniques.

To construct a full-color display, one needs to have polymers capable of emitting red, green, and blue lights. Although PF and modified PFs are the best known blue-light-emitting polymers, they tend to show so-called excimer emission in the green region in addition to the desired blue-light emission.[11,12] It is believed that excimer formation reduces not only the color purity but also the device efficiency.

In this investigation, we prepared the following three blue-light-emitting polymers and studied their luminescence properties, trying to understand how the comonomers units influenced their luminescence behavior. The structures of the repeating or corepeating units of the three polymers are known to be closely related to blue-light emitters:

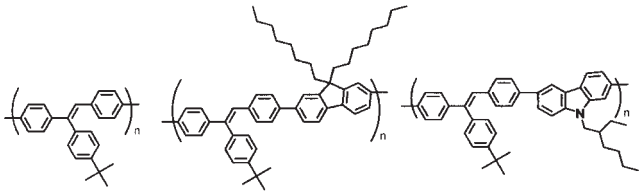

PBPV **P(DOF-PVP)** **P(EhCz-PVP)**

In addition, all of the polymers contained bulky pendants, which we hoped would reduce or eliminate the possibility for the formation of excimers.

RESULTS AND DISCUSSION

Synthesis of the monomers

The three monomers {1,2-bis(4-bromophenyl)-1-(4-*t*-butylphenyl)ethene (**A** or BPBPE), 9,9-dioctylfluorene-2,7-bis[4,4,5,5-tetramethyl-(1,3,2)-dioxaborate] (**B** or DOFBR), and *N*-(2-ethylhexyl)carbazole-3,6-bis[4,4,5,5-tetramethyl-(1,3,2)-dioxaborate] (**C** or EhCzBR)} were prepared with known synthetic methods, as shown in Scheme 1. **A** was prepared by a modified Wittig reaction[13,14] between 4-bromo-4′-*t*-butylbenzophenone (**1**)

Correspondence to: J.-I. Jin (jijin@korea.ac.kr).
Contract grant sponsor: Korea Science and Engineering Foundation through the Center for Electro- and Photoresponsive Molecules, Korea University.

Journal of Applied Polymer Science, Vol. 100, 307–317 (2006)

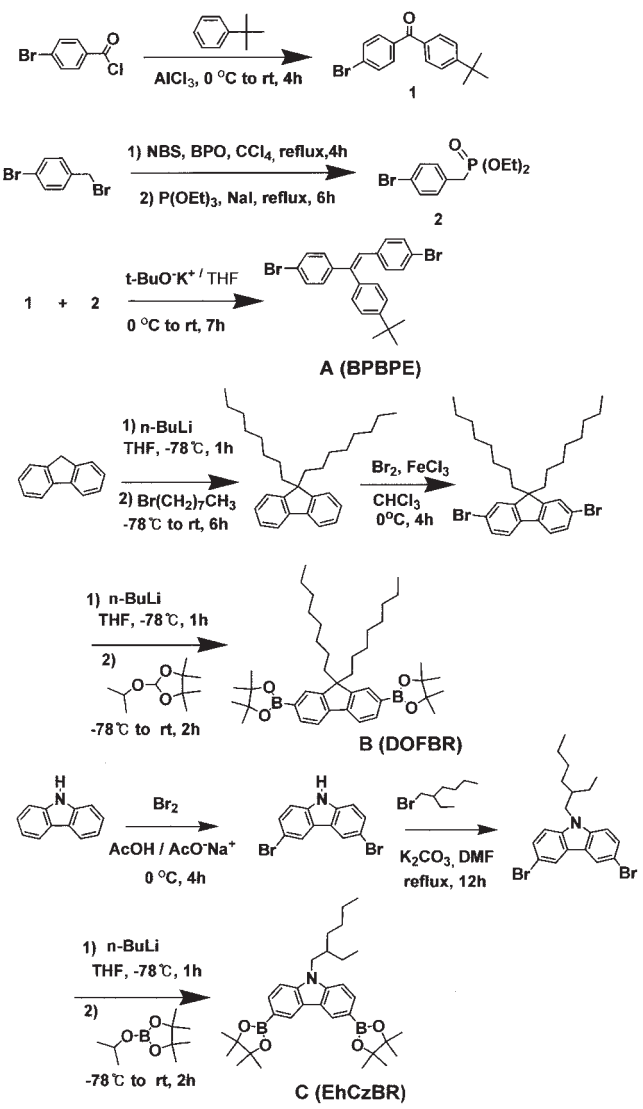

Scheme 1 Synthetic schemes of the monomers.

and *p*-bromobenzylphosphonate (**2**). The monomers **B** and **C** were bisboronic acids prepared starting from fluorene and carbazole, respectively, via the routes shown in Scheme 1.[15] The structures of the intermediates and the monomers were confirmed by Fourier transform infrared spectroscopy and ^{1}H-NMR spectroscopy and also by elemental analysis as described in the Experimental section. Monomer **A** was dissymmetrical, whereas **B** and **C** were symmetrical in structure. The dissymmetrical structure of monomer **A** was expected to bring about structural irregularities along the backbone because head-to-head and head-to-tail reactions were possible when it was involved in either homopolymerization or copolymerization.

Synthesis and general properties of the polymers

The homopolymer, poly{1,1′-biphenyl-4,4′-diyl-[1-(4-*t*-butylphenyl)]vinylene} (PBPV), was prepared by the oxidative self-condensation of **A** promoted by bis(1,4-cyclooctadienyl)nickel(0) and 1,4-cyclooctadiene. This reaction is called the Yamamoto reaction.[16] On the other hand, the other two alternating copolymers, poly((9,9-dioctylfluorene-2,7-diyl)-*alt*-{1,4-phenylene-[1-(4-*t*-butylphenyl)vinylene-1,4-phenylene]}) [P(DOF-PVP)] and poly([*N*-(2-ethyl)hexylcarbazole-3,6-diyl]-*alt*-{1,4-phenylene-[1-(4-*t*-butylphenyl)]vinylene-1,4-phenylene}) [P(EhCz-PVP)], were prepared in toluene by the Suzuki condensation[17,18] of compound **A** with either **B** or **C** (Scheme 2).

All three polymers were purified by Soxhlet extraction with methanol to remove impurities and catalysts. They were soluble at room temperature in organic solvents such as tetrahydrofuran (THF), methylene chloride (MC), and chlorobenzene.

Table I summarizes information on the molecular weights and glass-transition temperatures (T_g's) of the three polymers. The molecular weights determined by gel permeation chromatography (GPC) were not high [number-average molecular weight (M_n) = 5400–9100; weight-average molecular weight (M_w) = 7500–12,000]. The degree of polymerization (DP) ranged from 9 to 20. The polydispersity index (PDI = M_w/M_n) was rather low (1.3–1.6), which was probably due to the removal of low-molar-mass polymers by extraction with methanol.

The T_g values of these polymers varied widely: The homopolymer PBPV showed the highest T_g value of 212°C, whereas the dioctylfluorene copolymer P(DOF-PVP) exhibited the lowest T_g value (132°C). Although it is known that the T_g value of a polymer greatly depends on its chemical structure and molecular weight, the differences in the T_g value of these polymers can be correlated with the structures of the pendant groups. When compared with PBPV, the other two polymers bore long alkyl groups: P(DOF-PVP) carried two octyl groups on the nine position of the fluorene moiety, whereas P(EhCz-PVP) bore only one 2-ethylhexyl group on the nitrogen atom of the carbazole moiety. Therefore, the T_g value of P(EhCz-PVP) (180°C) was between the two extremes.

Ultraviolet–visible (UV–vis) absorption and PL characteristics

Figure 1 compares the UV–vis absorption and PL spectra of the three polymers in spin-coated thin (thickness = 200 nm) films. The wavelength of the excitation beam was 340 nm. The maximum absorption wavelengths for π–π^* transitions were not much different from each other, ranging from 350 nm for PBPV to 347 nm for the other two polymers. Their absorption edges were in the increasing order P(EhCz-PVP) [421 nm; bandgap energy (E_g) = 2.94 eV)], P(DOF-PVP) (429 nm; E_g = 2.89 eV), and PBPV (441 nm; E_g = 2.81 eV). This implies that the presence of the

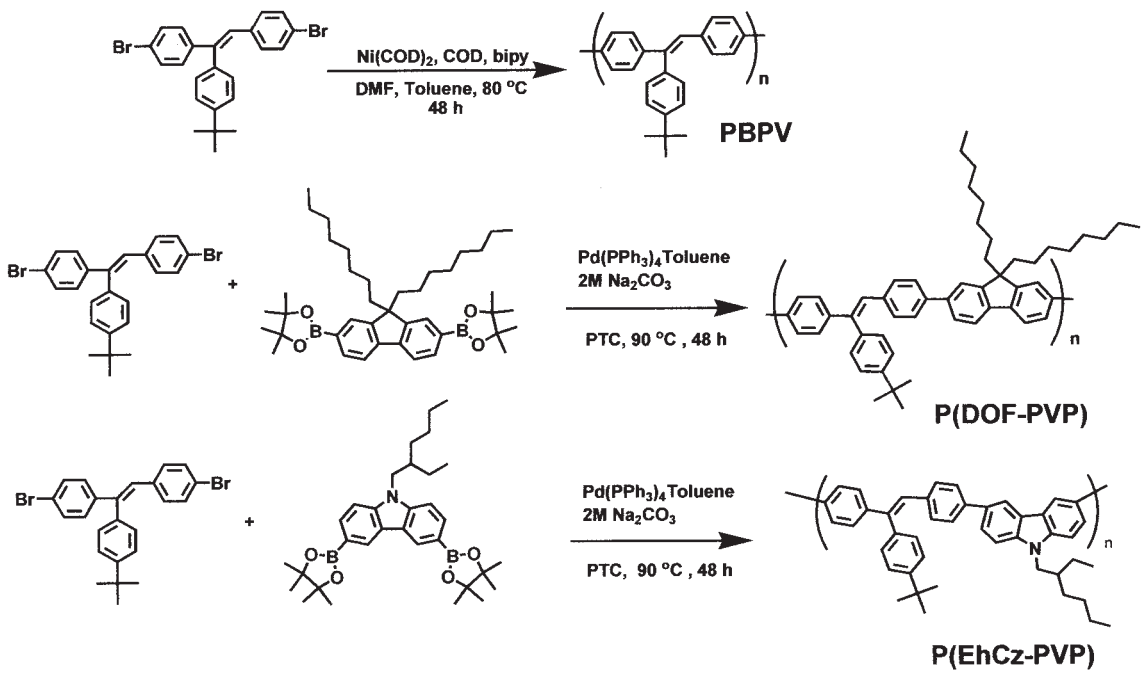

Scheme 2 Polymerization reaction schemes.

two comonomer units in the repeating unit diminished delocalization of π-electrons in the backbone, which led to elevated E_g's. The E_g value of P(EhCz-PVP), which was a little higher than that of P(DOF-PVP), was ascribed to the presence of the electronegative nitrogen atom in one of the structural units in the former.

As far as the PL properties (Fig. 1) of these polymers were concerned, they emitted blue light in thin films. Although their emission wavelength ranges did not vary much, the maximum emission wavelength of the films increased in the order P(DOF-PVP) (467 nm) < PBPV (474 nm) < P(EhCz-PVP) (482 nm). There was no indication of emission in the longer wavelength region from the excited complexes, such as excimers and exciplexes.

Table II compares the relative PL quantum efficiencies (QEs) of the polymers in solution (1×10^{-5} mol/L of the repeating unit) in chloroform and in thin films (200 nm thick). In both cases, P(DOF-PVP) exhibited the highest PL QE among the three polymers. The PL QEs of the films were in line with the external QEs of the LED devices fabricated with them, which is discussed later.

TABLE I
Molecular Weights[a] and T_g Values of the Polymers

Polymer	M_n	M_w	PDI	DP	T_g (°C)
PBPV	6,300	9,800	1.6	20	212
P(DOF-PVP)	9,100	12,000	1.3	11	132
P(EhCz-PVP)	5,400	7,500	1.4	9	180

[a] Molecular weights were measured by GPC in THF solution. Polystyrene was used for calibration.

EL properties

We constructed LED devices of the polymers with the configuration indium–tin oxide (ITO)/poly(ethylenedioxythiophene) doped with poly(styrene sulfonate) (PEDOT-PSS; Bayer, Leverkusen, Germany; 30 nm)/polymer (150 nm)/Li:Al (100 nm). We applied the conducting layer of PEDOT-PSS onto the ITO-coated glass (anode) to improve the hole injection into the light-emitting layer. A lithium/aluminum (0.3:99.7 by weight) alloy was evaporated onto the polymer

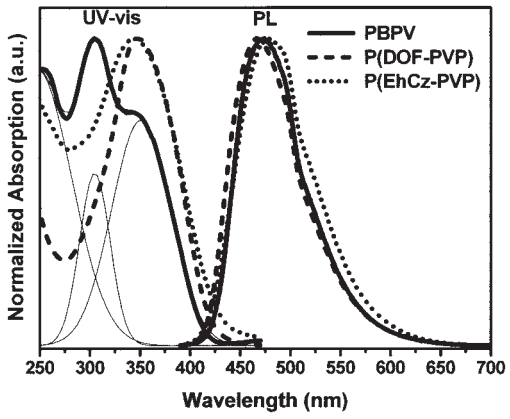

Figure 1 UV–vis absorption and fluorescence (PL) spectra of the polymer films (200 nm).

TABLE II
PL QEs of the Solutions and Films

Polymer	QE[a] (%) of the solution	QE[b] (200 nm) of the Film
PBPV	20.7	0.71
P(DOF-PVP)	29.5	1.43
P(EhCz-PVP)	15.5	1.00

[a] Coumarin307 was used as a standard material (QE = 72.4%).
[b] Relative value [normalized by the QE value of P(EhCz-PVP)].

layer to deposit the lithium cathode layer protected by aluminum. Among the three LEDs fabricated, we could obtain EL spectra (Fig. 2) only from P(DOF-PVP) and P(EhCz-PVP) but not from PBPV, whose EL emission was too weak to record. Figure 2 shows that the EL spectrum of P(DOF-PVP) was sharper and more in the blue-light region than that of P(EhCz-PVP). The wavelengths of maximum intensity of light emission for the two polymers were 450 and 476 nm, respectively.

The electrical characteristics of the devices are presented in Figure 3. According to the results shown in Figure 3, the device performance of P(DOF-PVP) was the best, whereas the PBPV device performed the worst. For the P(DOF-PVP) device, the current density (I) versus the applied electric field [V; Fig. 3(a)] and the light output (L) versus V [Fig. 3(b)] curves revealed more or less parallel increases in I and L values as we increased V. This implies that carriers injected by the electrodes were relatively efficiently used for light emission. The pallalelism between the I–V and L–V curves was the worst for the PBPV device. The device of P(EhCz-PVP) exhibited a far better pallalelism than the PBPV device, but it was a little worse than that of P(DOF-PVP). The threshold Vs of the devices varied from 1.4 MV/cm for the P(EhCz-PVP) device to 1.9 MV/cm for the P(DOF-PVP) device.

The maximum Ls of the devices were 0.02 μW at 1.9 MV/cm, 2 μW at 2.1 MV/cm, and 4.8 μW at 2.6 MV/cm, respectively, for the PBPV, P(EhCz-PVP), and P(DOF-PVP) devices. Figure 3(c) compares the dependence of the external QE of the three devices on I. The maximum external efficiency was 3×10^{-4}, 1.0×10^{-2}, and 1.5×10^{-2} %, respectively for the PBPV, P(EhCz-PVP), and P(DOF-PVP).

We determined the HOMO and LUMO levels of these polymers from their optical bandgaps and oxidation potentials obtained from cyclovoltammetry. The energy diagram shown in Figure 4 suggests that not only electron injection from the cathode to the emitting layer was easiest for P(DOF-PVP), but also the holes injected to the emitting layer from the anode were most efficiently trapped in the layer. In contrast, electron injection and hole blocking were least favorable for PBPV. The situation for P(EhCz-PVP) was between these two. This explains, at least partially, why the P(DOF-PVP) device performed best whereas the PBPV device performs the worst. In contrast, easier hole injection from the anode to the emitting layer was expected for PBPV than for the other two. These results demonstrated that easier electron injection to the emitting layer was more crucial for better device performance than hole injection, which has been ascertained by many other scientists.[19–21] In addition, Figure 5 shows that fluorescence decay in films (70–90 nm thick) was fastest for PBPV and slowest for P(DOF-PVP). The decay curves could be well fitted with a three-time constant model:

$$I(t) = A_1 e^{-t_1/\tau_1} + A_2 e^{-t_2/\tau_2} + A_3 e^{-t_3/\tau_3}$$

The results are summarized in Table III. When the data given in Table III are compared, it can be said that PL decay was slowest for P(DOF-PVP) among the three polymers, although P(EhCz-PVP) revealed the longest tail. Among the three, the PL decay behavior of P(DOF-PVP) and P(EhCz-PVP), however, was very similar. This observation provides us with an additional clue on the discriminating differences in the performance of the devices fabricated with these three polymers. It, however, should be pointed out that the maximum external QE of P(DOF-PVP) that we obtained was still significantly lower than that reported for poly(dioctylfluorene),[22] although the color purity was improved by suppression of the green band. Most probably, much more optimization of the device structure will be required to attain higher efficiency values.

Carrier mobility

We measured mobilities of the two types of carriers, that is, positive holes and negative electrons, for the

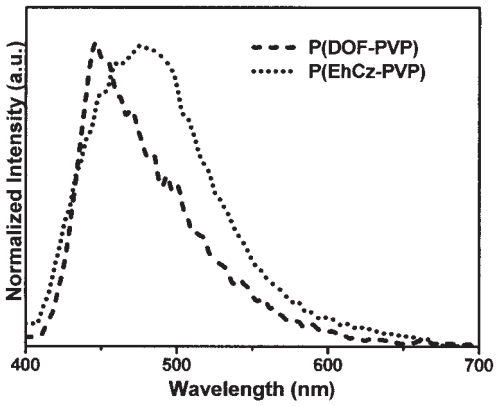

Figure 2 EL spectra of P(DOF-PVP) at 2.5 MV/cm and P(EhCz-PVP) at 2.2 MV/cm for the device of ITO/PEDOT (30 nm)/polymers (110–150 nm)/Li:Al (100 nm).

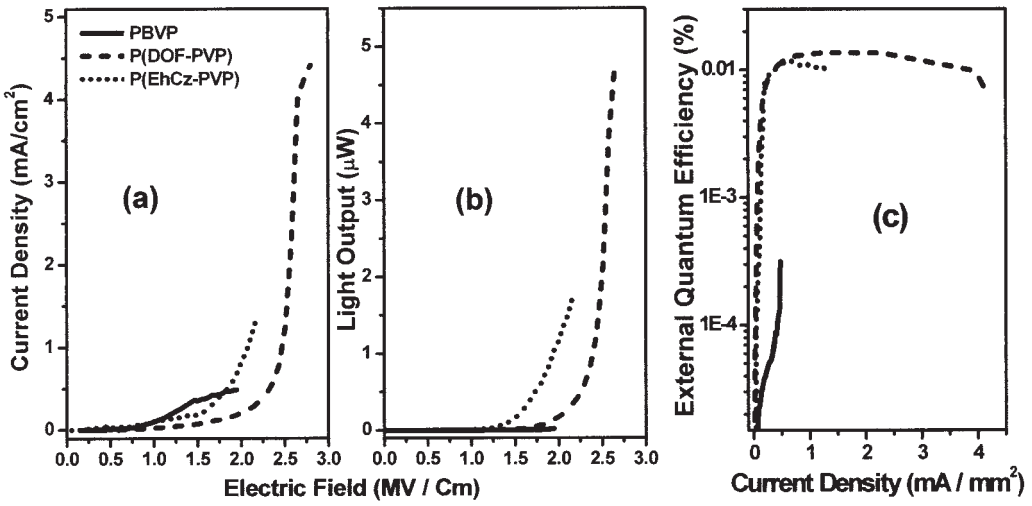

Figure 3 (a) I versus V, (b) luminance versus V, and (c) I versus external QE curves for the EL devices [ITO/PEDOT (30 nm)/polymers (110–150 nm)/Li:Al (100 nm)].

three polymers by the time-of-flight (TOF) method.[23] For the TOF measurements, devices with a configuration of ITO/polymer (200–460 nm thick)/Al (30 nm thick) were fabricated. Photogeneration of carriers was induced by an Nd-YAG laser light of 355 nm. Figure 6(a–f) shows profiles of the dependence of carrier current on time, and all the curves exhibited definitive inflection points, which made the estimation of carrier mobilities unequivocal. Table IV compares the estimation of carrier mobilities for positive holes (μ_h) and negative electrons (μ_e), of these three polymers. Among the three polymers, P(DOF-PVP) revealed the greatest balance in the mobility of carriers: μ_h/μ_e = 1.1. Moreover, the μ_h and μ_e were highest: $\mu_h = 5.6 \times 10^{-4}$ and $\mu_e = 5.2 \times 10^{-4}$ cm^2/V s. PBPV also showed a good balance in the mobility of carriers, μ_h/μ_e = 0.91. The mobility of the both carriers, however, was much slower. P(EhCz-PVP) exhibited the worst balance in the mobility of carriers, μ_h/μ_e = 0.34, although the carrier mobilities ($\sim 10^{-4}$ cm^2/V s) were faster than those for PBPV. It was rather surprising that the hole mobility of P(EhCz-PVP) was smaller than its electron mobility, despite the presence of the carbazole moieties along the backbone. However, μ_h of P(EhCz-PVP) (1.5×10^{-4} cm^2/V s) was more than 20 times μ_h of PBPV (6.7×10^{-6} cm^2/V s). Nevertheless, the best balance in the mobility of carriers must have been another important cause, in addition to its favorable electronic structures (HOMO and LUMO levels in Fig. 4), for the best EL performance of P(DOF-PVP) among the three polymers.

Recently, we prepared PPV derivatives bearing carbazole and phenyloxadiazole pendants, and their EL properties were studied.[9,24] Both polymers were green emitters and showed excellent external QEs, which could be explained by the balance in the mobilities of charge carriers.[25] The well-known PPV derivative, poly[2-methoxy,5-(2-ethylhexyloxy)-1,4-phenylenevinylene], however, revealed a much higher (ca. 100

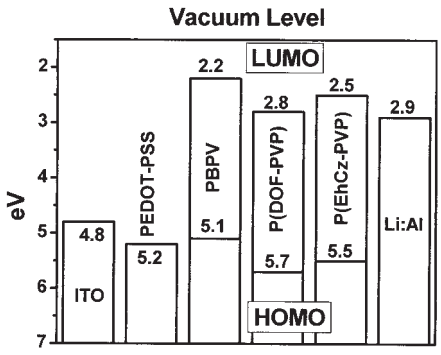

Figure 4 Electronic structures of PBPV, P(DOF-PVP), and P(EhCz-PVP).

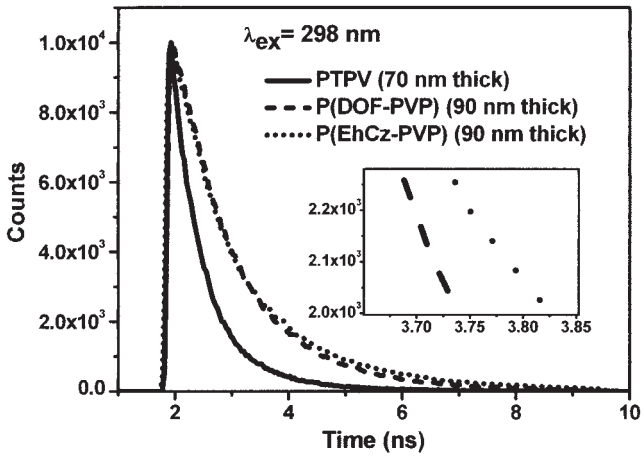

Figure 5 Time-resolved PL decay curves of the polymers.

TABLE III
PL Decay Parameters

Polymer	τ_1 (ns)	τ_2 (ns)	τ_3 (ns)	A_1	A_2	A_3
PBPV	0.57	0.19	1.64	0.22	0.18	0.019
P(DOF-PVP)	0.19	1.47	0.69	0.061	0.16	0.19
P(EhCz-PVP)	0.17	0.76	1.93	0.056	0.21	0.11

times) μ_h than μ_e.[26,27] μ_h[28] of poly(9,9-dioctylfluorene) was reported to be 8.5×10^{-3} $cm^2/V \cdot s$ at 10^4 V/cm, but electrons were too dispersive to measure their mobility.

CONCLUSIONS

We successfully prepared three new blue-light-emitting polymers containing substituted biphenylenevinylene units. All of the polymers did not exhibit the

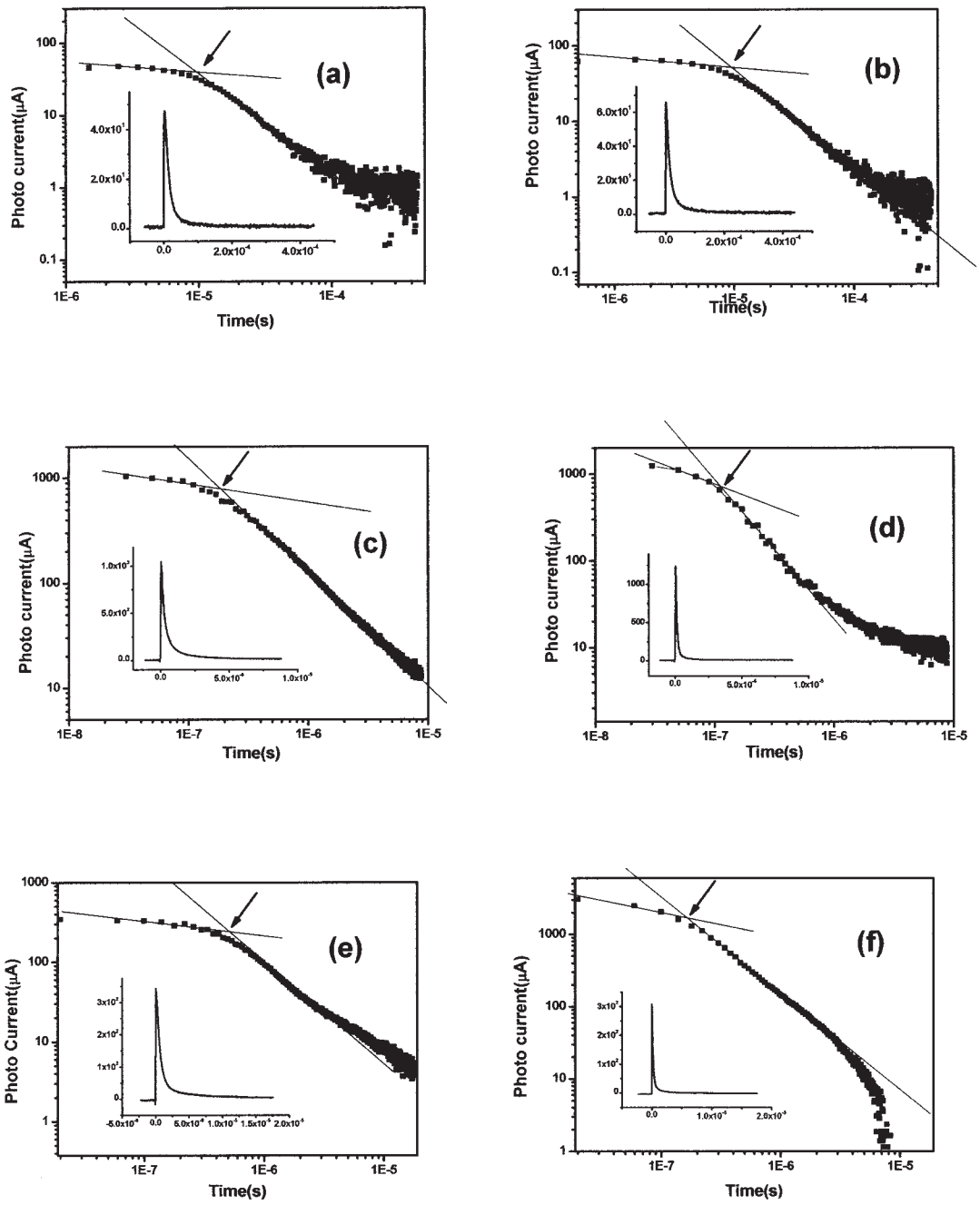

Figure 6 Double-logarithmic plots and double-linear plots (insets) of current versus time for the PBPV (a) μ_h and (b) μ_e, P(DOF-PVP) (c) μ_h and (d) μ_e, and P(EhCz-PVP) (e) μ_h and (f) μ_e. The transit times are marked on each double-logarithmic plot by an arrow.

TABLE IV
μ_h and μ_e Values of the Polymers

Sample	Thickness of the polymer film (nm)	μ_h (cm^2/Vs) (at electric field V/cm)	μ_e (cm^2/Vs) (at electric field V/cm)	μ_h/μ_e
PBPV	299	6.7×10^{-6} (4.7×10^5)	7.4×10^{-6} (4.7×10^5)	0.91
P(DOF-PVP)	235	5.6×10^{-4} (2.1×10^5)	5.2×10^{-4} (3.8×10^5)	1.1
P(EhCz-PVP)	216	1.5×10^{-4} (2.8×10^5)	4.4×10^{-4} (3.2×10^5)	0.34

formation of any intimate aggregates or excimers in the solid films, as evidenced by their UV–vis absorption and PL spectra. This was ascribed to the presence of bulky substituents along the chains. Among the three polymers, PBPV, P(DOF-PVP), and P(EhCz-PVP), the polymer [P(DOF-PVP)] with alternating sequences of the dioctylfluorene and biphenylenevinylene units revealed the best EL performance and also the highest PL efficiency in solution as well as in film. The favorable electronic structure (HOMO and LUMO levels), the longest PL lifetime, and the superior balance in carrier mobilities were major factors contributing to the better EL performance of P(DOF-PVP) among the three polymers reported in this investigation.

EXPERIMENTAL

Chemicals and instruments

All of the chemicals were obtained commercially from Aldrich Chemical Co., Inc. (Milwaukee, WI), Tokyo Kasei Kogyo (Tokyo, Japan), Strem Chemical (Newburyport, MA), or ACROS Organics (Geel, Belgium). They were analytical or higher grade and were used without further purification. Solvents to be used under anhydrous conditions were dried by standard methods. IR spectra were recorded on a Fourier transform infrared Bomem Michelson instrument (Quebec, Canada). ^{1}H-NMR spectra were recorded on a Varian Gemini 300 spectrometer (Palo Alto, CA). Elemental analyses were performed by the Korea Basic Science Institute, Seoul, Korea with a Flash EA 1112 series elemental analyzer (Milan, Italy).

Characterization and device fabrication

The molecular weights and molecular weight distributions of the polymers were determined by GPC. GPC analysis was conducted at 40°C with a Wyatt Dawn (Santa Barbara, CA) EOS system (London) equipped with Ultra-I-stragel columns with THF as the eluent at a flow rate of 0.5 mL/min and with polystyrene as the calibration standard. The T_g's of the polymers were studied under a nitrogen atmosphere on a Mettler (Greifensen, Germany) DSC 821^e instrument (OH). The heating and cooling rates were maintained at 10°C/min. Indium was used for temperature calibration and enthalpy changes involved in the phase transitions. The point where the initial slope change appeared in DSC thermogram was taken to be the T_g value.

The UV–vis absorption and PL luminescence spectra were recorded on an HP (Toronto, Canada) 8452A diode array spectrophotometer and an AMINCO-Bowman series 2 luminescence spectrometer (Rochester, NY), respectively, at room temperature. The current and luminescence intensity as a function of applied field were measured with an assembly consisting of a PC-based direct-current power supply (HP 6623A) and a digital multimeter (HP 34401). A light power meter (Newport Instruments, Plymouth, MA, model 818-UV) was used to measure the device L in microwatts.

We fabricated single-layer [ITO/PEDOT-PSS (30 nm)/EML (70 nm)/Li:Al] devices for the EL studies. ITO-coated glass slides with a sheet resistance of 25 Ω/cm^2 were patterned by the vapor of a mixed solution of HNO_3 and HCl at a volume ratio of 3:1.[29] The patterned ITO-coated glass slides were cleaned by sequential ultrasonication in acetone, methanol, and 2-propanol for 20 min and then dried in a stream of nitrogen. A hole-injecting layer, PEDOT-PSS (Bayer, Leverkusen, Germany), was spin-coated at a spin rate of 2000 rpm from its aqueous solution (0.8 wt %) onto the ITO substrates and cured at 160°C for 30 min in vacuo. Then a layer of polymer was spin-coated from its monochlorobenzene solution (2 wt %) at 1000 rpm. The thickness of the films was measured on a Sloan Dektak 3030 (Rocklin, CA) surface profilometer. The thickness of PEDOT-PSS was about 30 nm, and the thickness of the polymer layer was 70 nm, and the Li:Al alloy (Li 0.3 wt %) cathode electrode was deposited on the organic layers at a deposition rate of about 5 Å/s under a pressure of 1×10^{-5} torr with a VPC-260 vacuum coater (ULVAC, Kanagawa, Japan) and a CRTM-6000 thickness monitor (ULVAC). The active area of the device was 4.9 mm^2.

The cyclovoltammogram was obtained on an Amagel 2049 potentiostat and Power Lab system (4 sp) (PAR EG&G model 273A, Princeton, NJ). The redox behavior of the compounds was investigated with a standard three-electrode electrochemical cell in a 0.10*M* tetrabutylammonium tetrafluoroborate solution in acetonitrile at room temperature under nitrogen with a scanning rate of 20 mV/s. A platinum working electrode, counter electrode, and Ag/Ag^+ (0.01*M* in ACN) reference electrode were used.

The steady-state PL spectra were recorded with an excitation at 298 nm with a cw He:Cd laser. Fluorescence lifetimes of the spin-cast polymer films (70–90 nm thick) were measured by a time-correlated single-photon counting method.[30] The excitation source was a cavity-dumped picosecond dual-jet dye laser. To excite the sample, the dye laser pulse was frequency-doubled by a β-barium borate crystal. As for the excitation at 400 nm, the second harmonic from a femtosecond Ti:sapphire laser was used.

To measure charge carrier mobility, we fabricated devices as follows. A ITO-coated quartz plate with a sheet resistance of 15 Ω/cm^2 was used to coat polymer films. Polymeric layers were spin-coated on an ITO–quartz substrate. The thickness of the emitting layers was between 200 and 460 nm. The semitransparent aluminum electrode was deposited on the organic layers to a thickness of 30 nm at a deposition rate of about 2 Å/s under a pressure of 1×10^{-6} Torr with a VPC-260 vacuum coater (ULVAC) and a CRTM-6000 thickness monitor (ULVAC): ITO/sample (200–460 nm)/Al (30 nm). The active area of the device was 4.9 mm^2. The thickness of each layer was determined by a Tencor P-10 surface profiler (Tencor, Rocklin, CA).

To measure the carrier mobility of these materials, a conventional TOF measurement technique[23] was used. For optical excitation, a 7-ns pulse at $\lambda = 355$ nm (the third-harmonic Q-switched Nd-YAG laser, 10 Hz, Continuum) was used. The transient photocurrent was measured with a digital storage oscilloscope (LeCroy, Chestnut Ridge, NY 9361C, dual 300 MHz, Switzerland). Resisters from 50 Ω to 10 KΩ were used for photocurrent detection. We chose the resister's value considering the magnitude of the signal and RC time of the total circuit of a sample device. At first, the transient photocurrent profiles of *N,N′*-diphenyl-*N,N′*-di(*m*-tolyl)-benzidine (TPD) with a thickness of 900 nm [ITO/TPD (900 nm)/Al (30 nm)] was measured. The hole carrier transport appeared to be non-dispersive with a clear plateau and a subsequent current drop. The measured μ_h ($\approx 9 \times 10^{-4}$ $cm^2/V{\cdot}s$) was in a good agreement with the results of Naka et al.[23]

Synthesis of the monomers

The synthesis of the monomers is outlined in Scheme 1.

4-bromo-4′-*tert*-butylbenzophenone

To a solution of *t*-butylbenzene (13.4 g, 1.0×10^2 mmol) in MC, we added *p*-bromobenzoyl chloride (20.1 g, 9.2×10 mmol) at 0°C. Powdered anhydrous $AlCl_3$ (24.5 g, 1.8×10^2 mmol) was added in small portions to this solution with vigorous stirring for 3 h at 0°C. The mixture was subsequently allowed to warm to 25–30°C and was then stirred for 1 h. The reaction mixture was poured over crushed ice and extracted with MC. An organic layer was collected and dried over anhydrous magnesium sulfate. The solvent was distilled off to give the crude product, which was purified by column chromatography on silica gel with a mixture of hexane and ethyl acetate (1:10 v/v) as an eluent and recrystallized from ethanol. The product was a white solid (yield = 26.2 g, 68%):

^{1}H-NMR (300 MHz, $CDCl_3$, δ, ppm): 7.75–7.52 (m, 6H, Ar—*H*), 7.51 (d, 2H, Ar—*H*), 1.37 (s, 9H, —C(CH_3)$_3$. ANAL. Calcd for $C_{17}H_{17}BrO$: C, 64.37%; H, 5.40%. Found: C, 64.83%; H, 5.42%.

(4-bromobenzyl)phosphonic acid diethyl ester

p-Bromotoluene (10.00 g, 5.8×10 mmol), *N*-bromosuccinimide (12.49 g, 7.0×10 mmol), and benzoyl peroxide (1.40 g, 5.8 mmol) were dissolved in 200 mL of carbon tetrachloride, and then, the mixture was heated slowly to 76°C and refluxed for 4 h under a nitrogen atmosphere. After the completion of the reaction, the mixture was cooled to room temperature. The solvent was removed under a reduced pressure to obtain the crude product, which was further purified by column chromatography on a silica gel with hexane as an eluent. The yield of *p*-bromobenzyl chloride thus obtained was 12.5 g (89%). To a stirred suspension of NaI (6.74 g of previously washed compound with hexane, 5.8×10 mmol) in 20 mL of THF at 0°C added was 7.83 mL of triethylphosphite (7.48 g, 45 mmol) in 10 mL of THF. After 0.5 h, the solution of *p*-bromobenzyl bromide (7.50 g, 30 mmol) in 20 mL of THF was added dropwise to the previous solution over a period of 15 min, and then, the mixture was heated under reflux for 6 h. After it was cooled and quenched with cold water (30 mL), the mixture was extracted with ether (100 mL, three times). The ether layer was collected and dried over anhydrous magnesium sulfate. The solvent was removed to obtain a semisolid, which was purified by column chromatography on a silica gel with a mixture of hexane and ethyl acetate (1:4 v/v) as an eluent to obtain colorless needles (yield = 8.5 g, 92%):

^{1}H-NMR (300 MHz, $CDCl_3$, δ, ppm): 7.81 (d, 2H, Ar—*H*), 7.70 (m, 4H, Ar—*H*), 4.06 (q, 4H, —O$CH_2$$CH_3$), 3.22 (s, 2H, —$CH_2$—), 1.29 (t, 6H, —O$CH_2$$CH_3$). ANAL. Calcd for $C_{11}H_{16}BrO_3P$: C, 43.02%; H, 5.25%. Found: C, 42.92%; H, 5.21%.

BPBPE

To a stirred solution of 4-bromo-4′-*tert*-butylbenzophenone (**1:** 5.00 g, 1.6 × 10 mmol) and 4-bromobenzylphosphonic acid diethyl ester (**2:** 4.92 g, 1.6 × 10 mmol) in 20 mL of THF, 17 mL of 1.0*M* potassium *tert*-butoxide in THF was added slowly at 0°C via a syringe. After 1 h, the reaction mixture was heated to room temperature and maintained there for 6 h and quenched with cold water (100 mL). The mixture was extracted with ether (100 mL, three times). The ether layer was collected and dried over anhydrous magnesium sulfate. The solvent was removed to obtain a crude product, which was purified by column chromatography on silica gel with hexane as an eluent and recrystallized from hexane. The product was a white solid (yield = 6.20 g, 82%):

^{1}H-NMR (300 MHz, $CDCl_3$, δ, ppm): 7.47 (d, 2H, Ar—*H*), 7.35–7.19 (m, 6H, Ar—*H*), 7.07 (d, 2H, Ar—*H*), 6.89 (t, 3H, Ar—*H* and —*CH*═), 1.37 (s, 9H, —C(CH_3)$_3$. ANAL. Calcd for $C_{24}H_{22}Br_2$: C, 61.30%; H, 4.72%. Found: C, 61.90%; H, 4.81%.

DOFBR

This compound was prepared according to the procedures reported in the literature.[31]

3,6-dibromocarbazole

To a solution of carbazole (10.00 g, 6.0 × 10 mmol) in acetic acid and sodium acetate buffer solution was added 7.6 mL of bromine (23.85 g, 1.4 × 10^2 mmol) through a dropping funnel at 0°C. After the mixture was stirred for 4 h, we quenched the reaction by pouring 2*M* NaOH aqueous solution into the reaction mixture. The crude product was collected on a filter and washed with water and then recrystallized from ethanol. The product was a white solid (yield = 15.4 g, 79%):

^{1}H-NMR (300 MHz, $CDCl_3$, δ, ppm): 8.13 (d, 2H, Ar—*H*), 8.09 (br, 1H, N—*H*), 7.52 (dd, 2H, Ar—*H*), 7.31 (d, 2H, Ar—*H*). ANAL. Calcd for $C_{12}H_7Br_2N$: C, 44.35%; H, 2.17%; N, 4.31%. Found: C, 44.32%; H, 2.18%; N, 4.29%.

3,6-dibromo-*N*-(2-ethylhexyl)carbazole

To a solution of 3,6-dibromocarbazole (5.00 g, 1.5 × 10 mmol) in 40 mL of DMF were added 3.3 mL of 2-ethylhexyl bromide (3.57 g, 1.8 × 10 mmol) and K_2CO_3 (4.10 g, 3.0 × 10 mmol). The reaction mixture was refluxed for 12 h under a nitrogen atmosphere. The reaction mixture then was poured into distilled water. An aqueous solution was extracted with MC (3 × 100 mL). The organic layer was collected and dried over anhydrous magnesium sulfate. After the solvent was removed, the product was purified by column chromatography. The product was a white solid (yield = 5.8 g, 86%):

^{1}H-NMR (300 MHz, $CDCl_3$, δ, ppm): 8.10 (d, 2H, Ar—*H*), 7.54 (dd, 2H, Ar—*H*), 7.25 (dd, 2H, Ar—*H*), 4.07 (d, 2H, —OCH_2—), 1.97 [m, 1H, —$OCH_2CH(CH_2CH_3)CH_2CH_2CH_2CH_3$], 1.25–1.22 [br, 8H, —$OCH_2CH(CH_2CH_3)CH_2CH_2CH_2CH_3$], 0.88–0.82 [m, 6H, —$OCH_2CH(CH_2CH_3)CH_2CH_2CH_2CH_3$]. ANAL. Calcd for $C_{20}H_{23}Br_2N$: C, 54.94%; H, 5.30%; N, 3.20%. Found: C, 55.01%; H, 5.33%; N, 3.11%.

EhCzBR

n-Butyl lithium (2.5*M*, 3.8 mL, 1.5 × 10 mmol) in hexane was added slowly to a solution of 3,6-dibromo-*N*-(2-ethylhexyl)carbazole (3.00 g, 6.9 mmol) in 50 mL of dry THF.[32] After the reaction mixture was stirred at −78°C for 1 h, 2-isoproxy-4,4,5,5-tetramethyl-1,3,2-dioxaborolane (3.1 mL, 1.5 × 10 mmol) was added under a nitrogen atmosphere. The mixture was stirred for another 1 h at −78°C and then warmed to room temperature. After 1 h, we quenched the reaction by pouring the mixture into distilled water. The aqueous layer was extracted with ethyl acetate. The organic layer was collected and then dried over anhydrous magnesium sulfate. After the solvent was removed, the crude product was purified by recrystallization from methanol. The product was a white solid (yield = 2.0 g, 54%):

^{1}H-NMR (300 MHz, $CDCl_3$, δ, ppm): 8.66 (s, 2H, Ar—*H*), 7.90 (d, 2H, Ar—*H*), 7.38 (d, 2H, Ar—*H*), 4.19 (d, 2H, —OCH_2—), 2.05 [m, 1H, —$OCH_2CH(CH_2CH_3)CH_2CH_2CH_2CH_3$], δ 1.39 [s, 9H, —C($CH_3$)$_3$], 1.33–1.25 [br, 8H, —$OCH_2CH(CH_2CH_3)CH_2CH_2CH_2CH_3$], 0.90–0.82 [m, 6H, —$OCH_2CH(CH_2CH_3)CH_2CH_2CH_2CH_3$]. ANAL. Calcd for $C_{32}H_{47}B_2NO_4$: C, 73.33%; H, 8.92%; N, 2.64%. Found: C, 73.37%; H, 8.89%; N, 2.69%.

PBPV[16]

A Schlenk tube containing 6 mL of toluene, 6 mL of DMF, bis(1,5-cyclooctadieneyl)nickel(0) (0.314 g, 1.14 mmol), 2,2′-bipyridyl (0.178 g, 1.14 mmol), and 0.14 mL of 1,5-cyclooctadiene (0.123 g, 1.14 mmol; the latter three in a molar ratio of 1:1:1) was heated under an argon atmosphere to 80°C for 0.5 h. BPBPE (0.940 g, 2.0 mmol) dissolved in degassed toluene (3 mL) at 80°C was added to the previous solution. Polymerization was allowed to continue at 80°C for 48 h under an argon atmosphere. After the reaction mixture was cooled to room temperature, it was poured into a mixture of methanol and distilled water (10:1 v/v) while it was stirred. The polymer precipitate was collected on a filter. It was redissolved into chloroform and passed through Florisil to remove the catalyst

residues. The resulting polymer solution was collected, concentrated, and precipitated in methanol. The polymer precipitate was recollected on a filter followed by Soxhlet extraction with methanol to remove oligomers and catalyst residue (yield = 0.50 g, 81%).

^{1}H-NMR(300 MHz, $CDCl_3$, δ, ppm): 7.65–7.54 (br, 2H, Ar—*H*), 7.54–7. 25 (br, 7H, Ar—*H* and —*CH*═), 7.19–6.99 (br, 4H, Ar—*H*), 1.31 [s, 9H, —C(CH_3)$_3$]. ANAL. Calcd for $C_{24}H_{22}$: C, 92.86%; H, 7.14%. Found: C, 92.57%; H, 7.08%.

P(DOF-PVP)[17,18]

To a Schlenk tube was added tricaprylylmethylammonium chloride (Aliquot 336; ~20 wt % based on monomer), DOFBR (0.624 g, 1.0 mmol), BPBPE (0.470 g, 1.0 mmol), and 6 mL of toluene. The mixture was heated to 70°C to dissolve all of the monomers, and then, 4 mL of 2*M* Na_2CO_3 aqueous solution was added. The flask was then evacuated and filled with argon three times. $Pd(PPh_3)_4$ (1.1×10^{-2} g, 9.5×10^{-2} mmol) was added to the mixture under an argon atmosphere. The flask was again evacuated and filled with argon three times. The mixture was vigorously stirred at 90°C for 48 h under an argon atmosphere. After the reaction mixture was cooled to room temperature, it was poured into a mixture of methanol and distilled water (10:1 v/v) while it was stirred. The polymer precipitate was collected on filter. It was redissolved into chloroform and passed through Florisil to remove the catalyst residue. The resulting polymer solution was collected, concentrated, and precipitated in methanol. The polymer precipitate was recollected on a filter followed by Soxhlet extraction with methanol to remove oligomers and catalyst residue (yield = 0.52 g, 74%):

^{1}H-NMR (300 MHz, $CDCl_3$, δ, ppm): 7.70–7.56 (br, 4H, Ar—*H*), 7.54–7.42 (br, 2H, Ar—*H*), 7.28 (br, 5H, Ar—*H* and —*CH*═), 7.18 (br, 2H, Ar—*H*), 6.97 (br, 2H, Ar—*H*), 1.97–1.92 (br, 4H, —CH_2CHCH$_2$CH$_2$CH$_2$CH$_2$CH$_2$CH$_3$), 1.31 [s, 9H, —C(CH_3)$_3$], 1.00 (br, 24H, —CH_2*CHCH*$_2$*CH*$_2$-*CH*$_2$*CH*$_2$*CH*$_2$CH$_3$), 0.69 (br, 6H, —CH_2CHCH$_2$CH$_2$-CH$_2$CH$_2$CH$_2$*CH*$_3$). ANAL. Calcd for $C_{53}H_{62}$: C, 91.06%; H, 8.94%. Found: C, 90.97%; H, 8.92%.

P(EhCz-PVP)[17,18]

A mixture of EhCzBR (0.531 g, 1.0 mmol) and BPBPE (0.470 g, 1.0 mmol) was polymerized in the presence of $Pd(PPh_3)_4$ (1.1×10^{-2} g, 9.5×10^{-2} mmol) in the same manner as described previously for the preparation of P(DOF-PVP). The polymer was a light yellow fiber (yield = 0.45 g, 77%):

^{1}H-NMR (300 MHz, $CDCl_3$, δ, ppm): 8.34–7.19 (br, 2H, Ar—*H*), 7.62 (br, 4H, Ar—*H*), 7.40 (br, 2H, Ar—*H*), 7.24 (br, 7H, Ar—*H* and —*CH*═), 7.08 (br, 2H, Ar—*H*), 6.94 (br, 2H, Ar—*H*), 4.04 [br, 2H, —*CH*$_2$CH(CH$_2$CH$_3$)CH$_2$CH$_2$CH$_2$CH$_3$], 1.97 [br, 1H, —CH$_2$*CH*(CH$_2$CH$_3$)CH$_2$CH$_2$CH$_2$CH$_3$], 1.29 [br, 17H, —C(CH_3)$_3$ and —CH$_2$CH(*CH*$_2$CH$_3$)*CH*$_2$*CH*$_2$*CH*$_2$CH$_3$], 0.78 [br, 6H, —CH$_2$CH(CH$_2$*CH*$_3$)CH$_2$CH$_2$CH$_2$*CH*$_3$]. Anal. Calcd for $C_{44}H_{45}N$: C, 89.90%; H, 7.72%; N, 2.38%. Found: C, 89.77%; H, 7.76%; N, 2.40%.

Two of the authors (C.-G.K. and S.-H.J.) were the recipients of the Brain Korea 21 Scholarship from the Ministry of Education and Human Resources, Korea.

References

1. Burroughes, J. H.; Bradley, D. D. C.; Brown, A. R.; Marks, R. N.; Mackay, K.; Friend, R. H.; Burn, P. L.; Holmes, A. B. Nature 1990, 347, 539.
2. (a) Gustafsson, G.; Gao, Y.; Treacy, G. M.; Klavetter, F.; Colaneri, N.; Heeger A. J. Nature 1992, 357, 477; (b) Hwang, D. H.; Lee, J. I.; Cho, N. S.; Shim, H. K. J Mater Chem 2004, 14, 1026; (c) Kim, Y. H.; Lee, H. O.; Jung, S. O.; Kwon, S. K. Macromol Res 2003, 11, 194.
3. (a) Greenhan, N. C.; Moratti, S. C.; Bradley, D. D. C.; Friend, R. H.; Holmes, A. B. Nature 1993, 365, 628; (b) Jin, S. H.; Kim, M. Y.; Kim, J. Y.; Lee, K.; Gal, Y. S. J Am Chem Soc 2004, 126, 2474.
4. Grice, A. W.; Bradley, D. D. C.; Bernius, M.; Inbasekaran, M.; Wu, W. W.; Woo, E. P. Appl Phys Lett 1998, 73, 629.
5. Bernius, M.; Inbasekaran, M.; O'Brien, J.; Wu, W. Adv Mater 2000, 12, 1737.
6. Pogantsch, L. R. A.; de Freitas, P. P. S.; Scherf, U.; Gaal, M.; Zojer, E.; List, E. J. W. Adv Funct Mater 2003, 13, 597.
7. (a) Chung, S. J.; Jin, J.-I.; Kim, K. K. Adv Mater 1997, 9, 551; (b) Jin, S. H.; Kang, S. Y.; Kim, M. Y.; Chan, Y. U.; Kim, J. Y.; Lee, K.; Gal, Y. S. Macromolecules 2003, 36, 3841.
8. (a) Kim, K.; Hong, Y. R.; Lee, S. W.; Jin, J.-I.; Park, Y.; Sohn, B. H.; Kim, W. H.; Park, J.-K. J Mater Chem 2001, 11, 3023; (b) Cho, H. J.; Jung, B. J.; Cho, N. S.; Lee, J.; Shim, H. K. Macromolecules 2003, 36, 6704.
9. (a) Lee, D. W.; Kwon, K. Y.; Jin, J.-I.; Park, Y. Y.; Kim, R.; Hwang, I. W. Chem Mater 2001, 13, 565; (b) An, B. K.; Kim, Y. H.; Shin, D. C.; Park, S. Y.; Yu, H. S.; Kwon, S. K. Macromolecules 2001, 34, 3993.
10. Sohn, B. H.; Kim, K.; Choi, D. S.; Kim, Y. K.; Jeoung, S. C.; Jin, J.-I. Macromolecules 2002, 35, 2876.
11. Gaal, M.; List, E. J. W.; Scherf, U. Macromolecules 2003, 36, 4236.
12. List, E. J. W.; Guentner, R.; de Freitas, P. S.; Scherf, U. Adv Mater 2002, 14, 374.
13. Wittig, G.; Schöllkopf, U. Chem Ber 1954, 87, 1318.
14. Wittig, G.; Haag, W. Chem Ber 1955, 88, 1654.
15. Ranger, M.; Leclerc, M. Macromolecules 1999, 32, 3306.
16. Yamamoto, T. Prog Polym Sci 1992, 17, 1153.
17. Ishiyama, T.; Abe, S.; Miyaura, N.; Suzuki, A. Chem Lett 1992, 691.
18. Yang, J.; Jiang, C. Y.; Zhang, Y.; Yang, R. Q.; Yang, W.; Hou, Q.; Cao, Y. Macromolecules 2004, 37, 1211.
19. Wu, F. I.; Reddy, D. S.; Shu, C. F.; Liu, M. S.; Jen, A. K. Y. Chem Mater 2003, 15, 269.
20. Huang, B.; Li, J.; Shao, P.; Qin, J. G.; Jiang, Z. Q.; Yu, G.; Liu, Y. Q. Chem Lett 2004, 33, 1376.
21. Lee, T. H.; Dickson, R. M. J Phys Chem B 2003, 107, 7387.
22. Grice, A. W.; Bradley, D. D. C.; Bernius, M.; Inbasekaran, M.; Wu, W. W.; Woo, E. P. Appl Phys Lett 1998, 73, 629.
23. (a) Naka, S.; Okada, H.; Onnagawa, H.; Yamaguchi, Y.; Tsutsui, T. Synth Met 2000, 111–112, 331; (b) Miyabe, K.; Tada, K.; Onoda, M. Thin Solid Films 2003, 438–439, 248.

24. Jang, J. W.; Oh, D. K.; Lee, C. H.; Lee, C. E.; Lee, D. W.; Jin, J.-I. J Appl Phys 2000, 87, 3183.
25. (a) Jang, J. W.; Lee, C. E.; Lee, D. W.; Jin, J.-I. Solid State Commun 2004, 130, 265; (b) Kang, H. S.; Kim, K. H.; Kim, M. S.; Park, K. T.; Kim, K. M.; Lee, T. H.; Lee, C. Y.; Joo, J.; Lee, D. W.; Hong, Y. R.; Kim, K.; Lee, G. J.; Jin, J.-I. Synth Met 2002, 130, 279.
26. Inigo, A. R.; Tan, C. H.; Fann, W. S.; Huang, Y. S.; Perng, G. Y.; Chen, S. A. Adv Mater 2001, 13, 504.
27. Inigo, A. R.; Chiu, H. C.; Fann, W.; Huang, Y. S.; Jeng, U. S.; Hsu, C. H.; Peng, K. Y.; Chen, S. A. Synth Met 2003, 139, 581.
28. Redecker, M.; Bradley, D. D. C.; Inbasekaran, M.; Woo, E. P. Appl Phys Lett 1999, 74, 1400.
29. Nguyen, T. P. In Handbook of Luminescence, Display Materials, and Devices; Nalwa, H. S.; Rohwer, L. S., Eds.; American Scientific: Stevenson Ranch, CA, 2003; p 60.
30. Lakowicz, J. R. In Principals of Fluorescence Spectroscopy, 2nd ed.; Kluwer Academic–Plenum: New York, 1999; Chapter 4.
31. Chen, X.; Liao, J.-L.; Liang, Y.; Ahmed, M. O.; Tseng, H.-E.; Chen, S.-A. J Am Chem Soc 2003, 125, 636.
32. Perrin, D. D.; Armarego, W. L. F. In Purification of Laboratory Chemicals, 3rd ed.; Pergamon: New York, 1988.